Journal of Cytology & Histology

ISSN: 2157-7099

Boarelli et al., J Cytol Histol 2016, 7:2
DOI: 10.4172/2157-7099.1000412

Research Article Open Access

Simultaneous Study of Cholesterol and GM1 Ganglioside by Specific Probes: Lipid Distribution during Maturation, Capacitation and the Acrosome Reaction

Boarelli P*, Monclus M, Lancellotti TS, Cabrillana M, Simón L, Funes A and Fornés M

Mendoza Andrology Research Laboratory (MARL), Mendoza Histology and Embryology Institute (MHEI), Histology and Embryology Area, Medical Scooll, Cuyo National University, Argentina

Abstract

Lipid distribution has been extensively studied in the plasma membrane of the male gamete due to its relevant role in sperm physiology. However, there are controversial reports about their distribution. Because of different reports about this topic, the aim of this work was define cholesterol and GM1 ganglioside location by simultaneous detection during sperm maturation, capacitation and the acrosome reaction in CF1 mouse sperm. We observed that throughout the epididymis, cholesterol detected by filipin III or complex and GM1 ganglioside by cholera toxin, co-localized in the acrosomal domain of the head and midpiece of the flagellum. During sperm capacitation, a decrease of cholesterol can be observed like *diffuse* pattern on the whole head, while GM1 ganglioside was restricted to the apical acrosome. Capacitated sperm incubated with acrosome reaction inducers showed a diffuse location on the head with both probes after acrosomal exocytosis. Also, both probes did not show different locations on the flagellum. These findings indicate that cholesterol and GM1 ganglioside have a dynamic behaviour during the life of the sperm, which could indicate that a continuous assembly or disassembly of the lipid raft could be involved in the responsiveness of the sperm to different environments. Thus, during sperm capacitation and acrosome reaction there is a redistribution of the lipids. However, there are not apparent changes during sperm maturation. Cholesterol efflux, a characteristic event of sperm capacitation, could be analyzed through *diffuse* pattern described by filipin, and GM1 ganglioside patterns observed by the cholera toxin could be interesting when it is needed to evaluate sperm capacitation and the acrosome reaction in fixed sperm.

Keywords: Cholesterol; GM1 ganglioside; Lipid; Spermatozoa

Introduction

The plasma membrane is considered as a whole and it cannot assert that there is a random distribution of its components; in contrast, they are highly defined. Molecular association generates a heterogeneous plasma membrane, allowing them to establish scaffolding for a wide variety of cellular functions within different regions. These regions of membrane have been defined as microdomains or "rafts", and they are enriched in cholesterol (CHL), glycosphingolipids, sphingomyelin, glycosylphosphatidylinositol (GPI)-anchored proteins, and diverse signal transduction proteins [1]. Their organisation restricts the access of proteins in such a way that only those attached to lipid raft reside in them [2]. The male gamete membrane is an interesting model in the study of specific lipids and proteins. The spermatozoa have lipids and proteins that stabilize the cell during its transit through both the male and female genital tracts. A number of these molecules become attached to the sperm surface during its transit through the epididymal duct, whereas other factors become associated to the sperm surface during ejaculation, when sperm cells are mixed with secretor fluids (seminal plasma) from diverse accessory sex glands [3]. Mammalian sperm undergo morphological, biochemical and functional changes during epididymal transit, known as sperm maturation [4]. However, these sperm are unable to fertilize an oocyte, and they must undergo sperm capacitation in the female reproductive tract [5,6]. To acquire fertilizing capacity, male gamete need to be in contact with molecules present in the female. This results in hyperactivated motility because of changes in metabolism and intracellular signaling cascades and the sperm capacitation also results in the readiness of sperm cells to bind to the cumulus layer and the zona pellucid [7-9]. Besides changes in the flagellum, sperm capacitation is also related to the ability of spermatozoa to undergo the acrosome reaction. Although the acrosome reaction is needed for fertilization and initially this process, it is considered part of the capacitation process, and it is a post-capacitation event. Acrosome reaction is required for fertilization and it is considered part of the sperm capacitation, and these processes are temporally coordinated/activated by similar signaling pathways [10]. Lipid rafts are involved in physiological changes that occur during sperm maturation, capacitation and acrosome reaction, as relative amounts of these specific molecules, the re-positioning of antigens from one region to another and the exchange of proteins with epididymal fluid [9,11-13]. For example, CHL efflux is known to be an early event closely associated with signaling cascades correlated to an increase in protein tyrosine phosphorylation (p-Y) during sperm capacitation [7,14-16]. Although lipid rafts have been studied during sperm life, their organization and function remains a controversial topic. Several authors have reported different points of view regarding the existence of lipid rafts in nature, or if they represent an artifact induced by the applied methods for their study [17-21]. Fixed and live sperm has been demonstrated to have an acrosomal plasma membrane rich in CHL, while the postacrosomal plasma membrane is relatively poor and it appears to be conserved in mammals [22-25].

However, the location and the dynamic changes of ganglioside

***Corresponding author:** Paola Boarelli, Mendoza Andrology Research Laboratory (MARL), Mendoza Histology and Embryology Institute (MHEI), Histology and Embryology Area, Medical Scooll, Cuyo National University, 80 Del Libertador, Av. Gral. San Martín Park, Mendoza 5500, Argentina, Tel: +54 261 4494143 (7019); Fax +54 261 4494117 (7050); E-mail: pvboarelli@yahoo.com.ar

Received December 21, 2016; **Accepted** May 15, 2016; **Published** May 25, 2016.

Citation: Boarelli P, Monclus M, Lancellotti TS, Cabrillana M, Simón L, et al. (2016) Simultaneous Study of Cholesterol and GM1 Ganglioside by Specific Probes: Lipid Distribution during Maturation, Capacitation and the Acrosome Reaction. J Cytol Histol 7: 412. doi:10.4172/2157-7099.1000412

(GM1) still remain unclear and its behavior has been largely discussed because of the different results reported in the literature, which depend on the method used for its study. Previous reports have observed GM1 acrosomal distribution in live sperm at physiological temperature; while the postacrosomal location was found in dead or weakly fixed cells [20].

Another study suggests that GM1 is located in postacrosomal domain both in non-capacitated and in capacitated sperm. These results indicate that GM1 is restricted to the head, but during the acrosome reaction changes its distribution to the midpiece of the flagellum [26]. Other authors reported that GM1 is found in the midpiece, but not in the sperm head. Besides, GM1 has also been shown to cross from the tail to the head in capacitated cells [27]. In rat sperm, GM1 was observed in the postacrosome domains and then moved to the acrosome during capacitation [28]. Finally, in human sperm, GM1 has been reported to present a uniform distribution and this does not change during sperm capacitation [29]. However, these assays were performed below the physiological temperature and/or various fixing methods have been employed, both conditions could the cause of different reports. Visualization of these membrane domains in living cells is very valuable, but their study is technically difficult. Moreover, the use of fixed cells is an important tool in male reproduction research and/or in predictive diagnosis. The aim of this work is to define the simultaneous location of CHL and GM1 by epifluorescence microscopy, using specific lipid probes in spermatozoa under a *prefixative* condition. A *postfixative* condition was also used as an alternative way to study in living cells. In the present study, lipid rafts undergo changes across epididymal transit (maturation), sperm capacitation and acrosome reaction. Cholesterol maintains its acrosomal location in immature cells, whereas during sperm capacitation there was loss. Ganglioside GM1 during epididymal transit has an acrosome distribution similar to the CHL. After sperm capacitation, apical acrosomal location predominates for GM1. However, during acrosome reaction its apical acrosomal distribution disappears as well as isothiocyano-fluoresceinated *Pisum sativum* (Edible pea) agglutinin (FITC-PSA) signal, indicating acrosome exocytosis. Fluorescence patterns obtained by both probes could be used when it is necessary to evaluate sperm capacitation and acrosome reaction. Therefore, specific experiments were conducted to analyze the lipid changes during sperm maturation, capacitation and acrosome reaction, to contributing to the knowledge of sperm physiology.

Materials and Methods

Reagents and animals

Reagents were purchased from Sigma-Aldrich (Bs. As., Argentina) and Invitrogen (Molecular Probe Products, Bs. As., Argentina). Anti-phosphotyrosine (Anti-phosphotyrosine PY-20 Mouse Hybridone) and biotinylated anti-mouse IgG (Mouse ExtrAvidin Peroxidase Staining Kit) were provided by ICN and Sigma, respectively. Months old and body weight between 25 and 30 g. The animals were housed in a climate controlled room (12 h light: 12 h dark).

The protocol was supported by the Institutional Committee for Use of Laboratory Animals (ICULA - School of Medicine - National University of Cuyo).

Culture media

The culture medium was a modified Ringer, known as HM (25 mmol l^{-1} Hepes, 109 mmol l^{-1} NaCl, 4.77 mmol l^{-1}, KCl, 1.19 mmol l^{-1}, $MgSO_4.7H_2O$, 1 mg/mL glucose, 3.7 mL Na-lactate 60% syrup, 1.19 mmol l^{-1} KH_2PO_4) [30]. Immediately before sperm capacitation experiments, a capacitating medium (HMB) was prepared from HM, supplemented by addition of Ca^{2+} (1.7 mmol.l^{-}), pyruvate (1 mmol.l^{-}), $NaHCO_3$ (mmol.l^{-}) and bovine serum albumin fraction V (BSA; 3 mg/mL). Finally, the pH was adjusted to 7.3 with 10 mol l^{-1} OHNa [14,15].

Mouse sperm collection and samples preparation

Mice were sacrificed by cervical dislocation. Sperm from caput and cauda epididymis were obtained by cutting the epididymal tubules and swim out into 0.5 mL of HMB or HM media, for capacitating or non-capacitating conditions, respectively. Sperm suspension was diluted to a final concentration of 5-10 × 10^6 cells/ml in fresh medium and incubated for 90 min at 37°C in an atmosphere of 5% CO_2 in the air, maintaining a constant pH 7.4 [31].

Motility and sperm vitality

After incubation, sperm viability was evaluated by yellowish eosin staining (Eosin Y), following the method described in the World Health Organization Laboratory Manual for the Examination and Processing of Human semen [32]. Briefly, sperm from each incubation condition were mixed with equal amounts of 0.5% (w/v; final concentration) Eosin Y prepared in phosphate buffered saline (PBS: 0.01 mol l^{-1} phosphate buffer, with the addition of 0.137 mol l^{-1} NaCl and 0.0027 mol l^{-1} KCl). Sperm suspensions were observed under an optical microscope, and one hundred cells were counted, differentiating *unstained* (live) and *stained* (dead) sperm cells. This technique was also used to check the motility (progressive and *in situ*) expressed as percentage of motile sperm over 100 cells.

Tyrosine phosphorylation: sperm capacitation status

Tyrosine phosphorylation detected by immunoblot assay was used to establishing the sperm capacitation status [14,15]. Sperm aliquots under capacitating and non-capacitating conditions were concentrated by centrifugation at 800 *g* for 15 min at room temperature, washed twice in PBS containing 0.2 mmol l^{-1} Na_3VO_4 (unspecific phosphatase inhibitor). These aliquots were resuspended in sampler buffer (25 mmol l^{-1} Tris, 0.5% SDS and 5% glycerol, pH 6.8) without β-mercapto-ethanol [33], and boiling for 10 min. After centrifuging at 9,000 *g* for 15 min, the supernatant was recovered and frozen until use.

Total protein extracts were supplemented with 5% β-mercaptoethanol (v/v, final concentration) and boiled for 10 min. Proteins were subjected to SDS-PAGE, using 10% mini-gels and performed for 120 min at 100 mV in electrophoresis equipment Mini-protean II (Bio-Rad, Hercules, CA). Protein extracts loaded per lane were equivalent to 5 - 10 × 10^6 sperm. Molecular weight markers (Bio-Rad, Hercules, CA) were run in parallel.

After electrophoresis, proteins were transferred to 45 µm nitrocellulose membrane (Bio-Rad Hercules, CA) in Electrophoretic Blotting Systems (Bio-Rad, Hercules, CA) for 60 min at 70 mV at room temperature [34]. Nonspecific reactivity was blocked by overnight incubation in blocking buffer prepared with 3% Teleostian fish gelatin (v/v) dissolved in washing buffer (TTBS: Towbin´s buffer saline plus 0.1% Tween 20) [14,15].

Immunodetection was performed at room temperature for 1 h with the monoclonal anti-phophotyrosine antibody (clone PY20, ICN Biomedicals) 1:5,000 in TTBS. Post-incubation membranes were washed three times in TTBS. Biotin-conjugated anti-mouse IgG (Sigma-Aldrich) was used as secondary antibody (1:1,250) and horseradish peroxidase-conjugated extravidine (Sigma) was added (1:750), both were placed in blocking buffer with a period of incubation

of 1 h at room temperature. Excess of first and second antibodies was washed three times in TTBS. Detection was accomplished with an enhanced chemiluminescence system (ECL; Amersham Biosciences) and subsequent exposure to Eastman Kodak Co. XAR film for 5-30 s.

Cholesterol and GM1 ganglioside detection by filipin and cholera toxin

Lipids were located by specific probes: filipin complex or filipin III (FIL) for CHL and cholera toxin subunit beta AlexaFluor 594 conjugate (CTB) for GM1. The methodology is based on protocols selected from literature and preliminary experiments [27,35].

FIL stock solution (7.6 mmol l^{-1}) and *CTB stock solution* (1.8×10^{-3} mmol l^{-1}) were prepared dissolving FIL in dimetyl-sulfoxide (DMSO) and CTB in PBS, respectively. Both solutions were stored in the dark at -20°C in aliquots for single use under a nitrogen atmosphere.

The study of both lipids was performed under *prefixative* and *postfixative* conditions.

In *prefixative* conditions, capacitated and non-capacitated sperm from cauda and caput epididymis were fixed for 30 min at room temperature with 4% (w/v) paraformaldehyde (PF) in PBS prepared at the time, pH 7.4. Then, spermatozoa were washed by centrifugation at 800 *g* for 15 min at room temperature to remove the excess of PF and then resuspended in PBS [25,35-39].

Filipin (0.15 mmol l^{-1} in PBS) and CTB (1.8×10^{-4} mmol l^{-1} in PBS) were applied sequentially to the spermatozoa for 60 and 30 min, respectively. This lipid detection protocol was carried out in the darkness at room temperature in a moisture chamber.

In *postfixative* condition, capacitated and non-capacitated sperm from cauda and caput epididymis were previously treated with specific probes, and then fixed for 30 min at room temperature with 4% (w/v) PF in PBS. The final concentration of each specific probe and incubation times were the same as those described above.

All samples were analyzed by phase contrast and fluorescence microscopy (see below). Samples without treatment with specific probes were tested to check the possibility of spurious signal.

Lipid specific probes and fluorescence patterns

Several authors have divided the sperm plasma membrane into five domains known as the acrosome, the equatorial segment, the postacrosome, the midpiece and the principal piece [22,40-42]. In view of these plasma membrane domains, fluorescence patterns were defined for both specific probes independently of the incubation/treatment conditions: *diffuse* pattern with weak signal on the whole head (Figure 1a), *acrosomal* pattern (Figure 1b), *postacrosomal* pattern (Figure 1c) with strong fluorescence in acrosome and postacrosome domains, respectively, *acrosomal-cap* with intense fluorescence signal on apical acrosomal region and weak or no label in the equatorial segment and postacrosome domain (Figure 1d), and *acrosomal-cap/postacrosomal*, fluorescence signal localized in apical acrosomal region and postacrosome domain (Figure 1e). These fluorescence patterns were then used to rate and quantify the location of CHL and GM1 in sperm plasma membrane.

Induction of acrosome reaction

Progesterone (PG) (1 mmol l^{-1}) and calcium ionophore (A23187) (2 mmol l^{-1}) in DMSO were used to induce acrosome reaction [43-45]. Ten µmol l^{-1} of PG or A23187 (final concentration) were added to capacitated sperm, and incubated for 15 min at 37°C in an atmosphere of 5% CO_2 in air. Basal groups were assayed without inducing reagents or with the only addition of DMSO (1:100).

After incubation and centrifugation at 800 *g* for 15 min at room temperature, samples were fixed for 30 min at room temperature with 4% (w/v) PF in PBS, pH 7.4. Sperm were washed in PBS to remove the excess of PF and stored at 4°C until use.

Evaluation of acrosome reaction by coomassie blue staining

Coomassie Blue staining was performed to assess acrosome reaction status in capacitated cauda sperm [46]. Capacitated sperm under acrosome reaction induced were sequentially treated for 5 min with distilled water, methanol, and a second wash with distilled water. Samples were incubated with a 0.22% (w/v) Coomassie blue G-250 in methanol (50%) and glacial acetic acid (10%) at room temperature for 2 min, and mounted with 90% (v/v) glycerol in PBS. Three hundred cells were recorded considering the presence (no reacted) or absence (reacted) of characteristic dark blue acrosomal-cap.

Lipid rafts and acrosome reaction

In order to assess the relationship between the lipid rafts and acrosome reaction, capacitated sperm from cauda epididymis subjected to induction with PG and/or A23187 were treated with lipid specific probes and FITC-PSA.

Specific probes for CHL (FIL) and GM1 (CTB) were used as previously described. Thereafter, sperm suspensions were incubated with 50 ug/ml of FITC-PSA in PBS for 60 min at room temperature in a moisture chamber in darkness. Samples were examined by epifluorescence microscopy [47,48]. Non-capacitated sperm from cauda epididymis were treated too with lipid probes and FITC-PSA under equal conditions.

Microscopy and image collection and processing

All experiments were analyzed by phase contrast and fluorescence microscopy using an Olympus FV10-ASW confocal microscope (New York, USA). For each treatment, cells were counted and categorized into different fluorescence patterns (see results).

Statistical analysis

All experiments were repeated at least three times in each incubation condition. Measurements were performed in triplicate and results were expressed as means ± S.E.M. Statistical differences between treatment groups were evaluated by two-way analysis of variance (ANOVA), using Bonferroni´s post-test. Differences were considered statistically significant at $p<0.05$ and $p<0.01$. Statistical analysis was performed using the *GraphPad Prism* 4 software (http//www.graphpad.com/prism/Prism.htm, San Diego, CA, USA).

Results

Vitality and motility control

For the present work, CF1 mice were selected due to their stability on spermatic parameters. Eosin test revealed high sperm viability (70.1% ± 9.7) [30]. After incubation and centrifugation treatments, vitality was again evaluated (64.6% ± 8.3). No statistic differences between both assays ($p>0.05$) were observed. Microscopic evaluation of sperm motility showed high and rapid progressive motility (~60%) prior to each experimental condition (data not shown). Samples that showed a low percentage of progressive motile sperm or eosin test below the values stated were discarded.

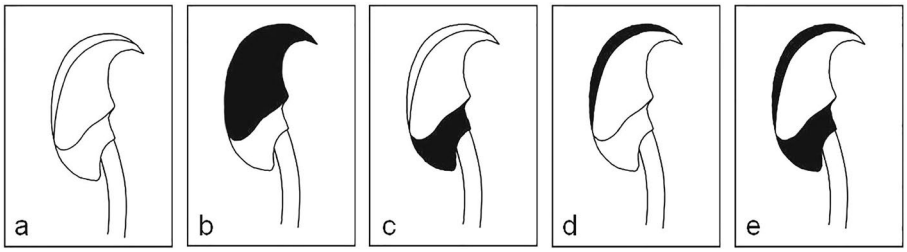

Figure 1: Sperm capacitation status by western blot analysis of tyrosine phosphorylated proteins obtained from non-capacitating (NC) and capacitating (C) experimental conditions. Only cauda sperm incubated in the capacitating medium presented immunoreactivity. Caput incubated under both conditions and cauda sperm incubated under non-capacitating condition did not show phosphotyrosine activity.

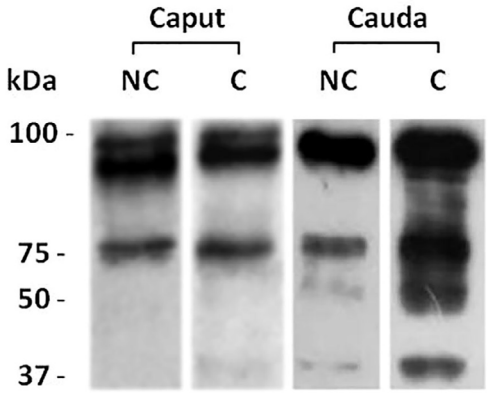

Figure 2: Fluorescence patterns on the head of spermatozoa established by lipid specific probes: *diffuse* (a), *acrosomal* (b), *postacrosomal* (c), *acrosomal-cap* (d), and *postacrosomal/acrosomal-cap* (e).

	Basal		DMSO		PG		A23187	
Reacted sperm (unstained acrosome domain)	8.5	± 0.5^{a}	12.5	± 1.2^{b}	16.3	± 2.5^{abc}	50.2	± 1.4^{abc}

Table 1: Control of induced acrosome reaction in capacitated cauda sperm by Coomassie blue staining method.
The results are expressed as a mean of percentages ± S.E.M. Superscript ^{a} represent statistical differences between basal *vs.* progesterone (PG) (p<0.05) and calcium ionophore (A23187) (p<0.001). Superscript ^{b} represent statistical differences between DMSO *vs.* progesterone (PG) (p<0.05) and calcium ionophore (A23187) (p<0.001). Superscript ^{c} represent statistical differences between PG *vs.* A23187 (p<0.05). No statistical significant difference (p>0.05) between the basal vs. DMSO.

Sperm capacitation: tyrosine phosphorylation

In order to establish capacitation status, tyrosine phosphorylated proteins were examined in spermatozoa from each incubation condition. Tyrosine phosphorylation was revealed by western blot on total sperm protein extracts. After 1 h of incubation under capacitating conditions, only sperm from cauda epididymis presented phosphotyrosine immunoreactivity. In contrast, caput and cauda epididymal spermatozoa, incubated in non-capacitating conditions, did not show phosphotyrosine activity. A similar result was observed in samples from caput sperm even when they were incubated in the capacitating medium. The protein bands obtained are those expected for this specie (Figure 2).

Acrosome reaction and coomassie blue staining

Sperm capacitation status can be established through induced acrosome reaction, because non capacitated sperm and immature sperm (caput sperm) not support acrosome exocytosis. Thus, the acrosome reaction in capacitated spermatozoa was determined by Coomassie blue staining method. Samples from capacitated cauda spermatozoa without induction treatment (basal group) were statistically significantly lower than those treated with PG (p<0.05) and A23187 (p<0.01). Dimetyl-sulfoxide control did not show any difference compared with basal group (p>0.05) (Table 1). These results were similar to previous reports [49].

Lipid specific probes and fluorescence patterns

For study to lipid rafts, CTB and FIL were employed to label the GM1 and CHL, respectively. Considering the reference patterns described previously, spermatozoa incubated with CTB presented *diffuse* (Figure 3Aa), *acrosomal* (Figure 3Ab) and *acrosomal-cap* (Figure 3Ac) as principal fluorescence patterns, while those incubated with FIL showed *diffuse* (Figure 3Bd) and *acrosomal* patterns (Figure 3Be).

Fluorescence in the *midpiece* of the flagellum and the *cytoplasmic droplets* were characteristically stronger than the fluorescence in the *principal piece*. Interestingly, this phenomenon was observed with both specific probes, and they showed the same patterns independently of experimental conditions (data not shown).

Samples without specific probes treatment (autofluorescence) showed a very weak signal (Figure 3C).

Cholesterol and GM1 ganglioside distribution in *prefixed* spermatozoa

The location of the CHL in caput sperm presented predominantly an *acrosomal* pattern (Ac) under non-capacitating conditions (Figure 4A, white bars) and capacitating conditions (Figure 4A, black bars).

Non capacitated cauda sperm showed an *acrosomal* pattern similar to spermatozoa from caput epididymis (Figure 4B, white bars). However capacitated cauda sperm showed a *diffuse* pattern (Figure 4B, black bars). These results indicate a loss of CHL during capacitation in cauda sperm as it was reported by others authors [14,16,20] while CHL in caput sperm (immature) not presented modifications under any condition.

The study of GM1 was more complex than the CHL because several fluorescence patterns were observed by epifluorencence microscopy. Sperm from caput (Figure 4C) and cauda (Figure 4D) epididymis subjected to non-capacitating conditions (white bars) and treated with CTB showed predominantly *acrosomal* patterns. These results could indicate that GM1 did not modify its distribution during epididymal transit.

Interesting *acrosomal* pattern (Ac) did not change in the immature sperm although under the capacitating conditions (Figure 4C, compare white and black bars). However cauda sperm presented predominantly *acrosomal-cap* pattern (ACap) after the *in vitro* capacitation (Figure 4D, black bars).

These results taken together suggest that GM1 was restricted to a narrow location over the acrosome (*acrosomal-cap* pattern) after *in vitro* sperm capacitation in prefixed sperm.

Cholesterol and GM1 ganglioside distribution in *postfixed* spermatozoa

Postfixed spermatozoa from caput epididymis under non-

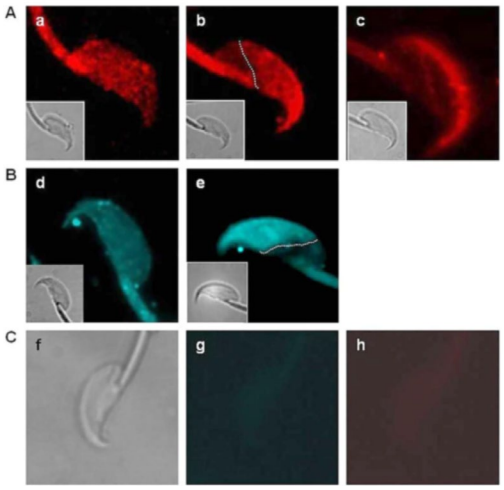

Figure 3: Principal fluorescence patterns to GM1ganglioside and cholesterol by CTB (A) and FIL (B) probes, respectively. Note *diffuse* (a and d) and *acrosomal* (b and e) patterns for both probes and an additional *acrosomal-cap* (c) pattern in sperm labeled by CTB. Insets show the corresponding phase contrast photomicrographs. Autofluorescence control (C) in spermatozoa without specific probes treatment, phase contrast (f) and fluorescence images (g and h).

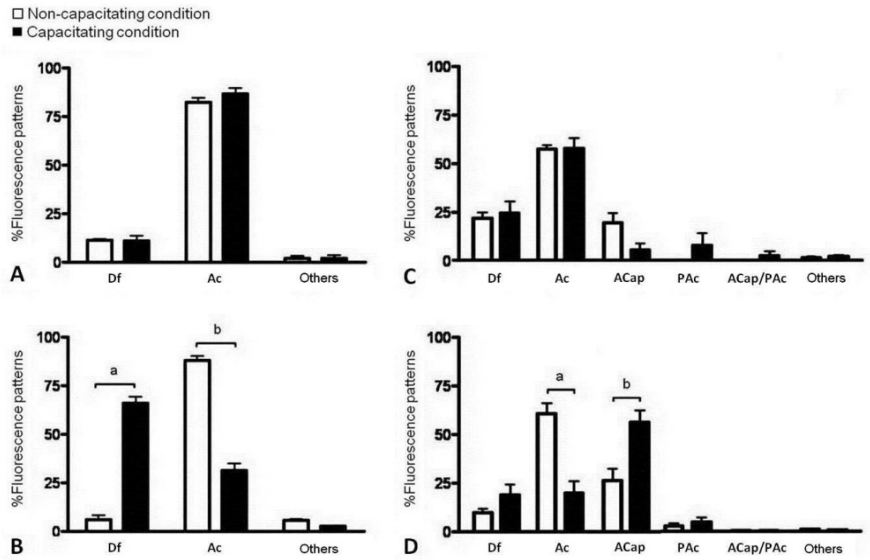

Figure 4: Cholesterol and GM1ganglioside in *prefixed* sperm by FIL and CTB probes, respectively. Cholesterol in caput sperm (A), show a predominantly *acrosomal* pattern (Ac), independently of incubation conditions (white and black bars). Between non-capacitated (white bars) and capacitated (black bars) cauda sperm (B) there was a change from *acrosomal* to *diffuse* pattern (Df). GM1 ganglioside in caput sperm (C) subjected to non-capacitating (white bars) or capacitating (black bars) conditions showed principally *acrosomal* patterns (Ac). Cauda sperm (D) incubated in non-capacitating conditions (white bars) showed *acrosomal* pattern (Ac), while capacitated cells (black bars) present *acrosomal-cap* pattern (ACap). Df: *diffuse*; Ac: *acrosomal*; ACap: *acrosomal-cap*; ACap/PAc: *acrosomal-cap/postacrosomal*; PAc: *postacrosomal*. Results are expressed as a mean of percentages ± S.E.M. Superscripts [a] and [b] represent statistical differences ($p<0.001$).

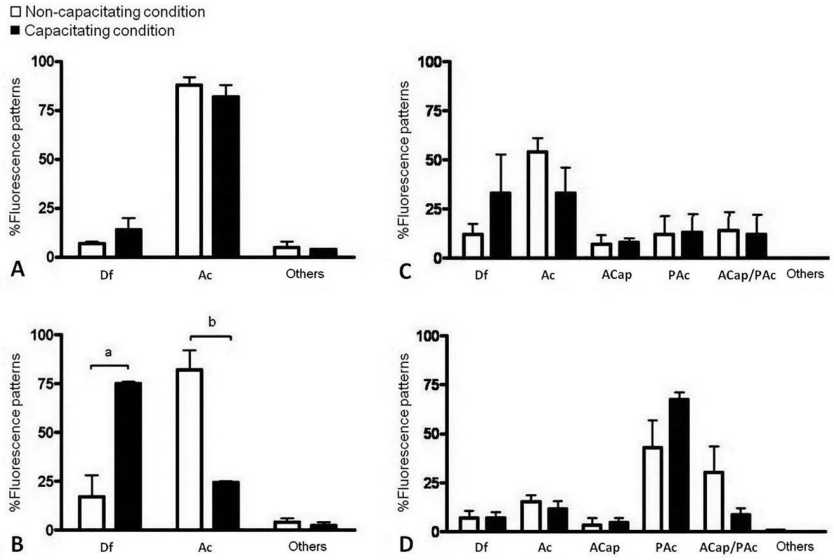

Figure 5: Cholesterol and GM1ganglioside in *posfixed* sperm by FIL and CTB probes, respectively. Cholesterol in caput sperm (A), show a predominantly *acrosomal* pattern (Ac), independently of incubation conditions (white and black bars). Between non-capacitated (white bars) and capacitated (black bars) cauda sperm (B) there was a change from *acrosomal* to *diffuse* pattern (Df). GM1 ganglioside in caput sperm (C) subjected to non-capacitating (white bars) or capacitating (black bars) conditions showed principally *acrosomal* patterns (Ac). Cauda sperm (D) incubated in both conditions (white and black bars) showed *acrosomal-cap/postacrosomal* (ACap/PAc) and *postacrosomal* patterns (PAc). Df: *diffuse*; Ac: *acrosomal*; ACap: *acrosomal-cap*; ACap/PAc: *acrosomal-cap/postacrosomal*; PAc: *postacrosomal*. Results are expressed as a mean of percentages ± S.E.M. Superscripts [a] and [b] represent statistical differences (p<0.001).

Fluorescence patterns	Non-capacitating condition		Capacitating condition		PG		A23187	
Df	9.7	± 2.1[a]	18.8	± 5.4[ac]	45	± 0.5[abc]	63	± 1.0[abc]
Ac	60.2	± 5.3[a]	19.8	± 6.1[ac]	3.5	± 2.0[abc]	1.5	± 1.5[abc]
ACap	26.2	± 5.9[a]	55.6	± 6.3[ac]	48.5	± 0.5[abc]	33.5	± 3.5[abc]
ACap/PAc	2.6	± 1.4	4.8	± 2.2	2	± 2.0	1.5	± 0.5
PAc	0.3	± 0.3	0.5	± 0.2	1	± 1.0	0.5	± 0.5
Others	1	± 0.5	0.6	± 0.4	0	± 0.0	0	± 0.0

Table 2: GM1 ganglioside fluorescence patterns detected by the CTB probe in *prefixed* cauda sperm subjected to sperm capacitation and the acrosome reaction by progesterone (PG) and calcium ionophore (A23187) induction. The results are expressed as a mean of the percentages ± S.E. Df: *diffuse*; Ac: *acrosomal*; ACap: *acrosomal-cap*; ACap/PAc: *acrosomal-cap/postacrosomal*; PAc: *postacrosomal*. Superscript [a] represent statistical differences between Non-capacitating conditions *vs.* Capacitating condition, progesterone (PG) and calcium ionophore (A23187) (p<0.001). Superscript [b] represent statistical differences between PG *vs.* A23187 (p<0.001). Superscripts [c] represent statistical differences between Capacitating condition *vs.* PG (p<0.01) and A23187 (p<0.001).

capacitating and capacitating conditions presents principally a *acrosomal* fluorescence pattern for CHL by FIL probe (Figure 5A, white and black bars). Similar result could be observed in capacitated sperm from cauda epididymis (Figure 5B, white bars). Moreover, sperm from cauda epididymis showed a *diffuse* pattern when they were incubated under capacitating conditions (Figure 5B, black bars). Thus, independently of fixative protocol applied and the incubation conditions, CHL distributions show the same pattern in *prefixed* and *postfixed* epididymal sperm (Compare Figures 4A, 4B with Figure 5A and 5B).

GM1 ganglioside in *postfixed* caput spermatozoa showed the same *acrosomal* pattern (Figure 5C, white and black bars) as the *prefixed* cells in non-capacitating and capacitating conditions (compare Figure 4C with Figure 5C, white and black bars). However, *postacrosomal* (PAc) and *acrosomal-cap/postacrosomal* (ACap/PAc) were the predominant fluorescent patterns observed in *postfixed* capacitated and non capacitated cauda sperm (Compare Figures 5C and 5D, white and black bars). Thus, under this *postfixation* protocol, GM1 presents *postacrosomal/acrosomal* cap and *acrosomal cap* pattern only in capacitated cauda sperm. These results suggest that GM1 has different location when the labelling method is performed after fixation (*postfixed* spermatozoa).

Lipids and acrosome reaction in *prefixed* capacitated spermatozoa

Mammalian male gamete undergoes acrosome reaction when sperm capacitation occurs. Besides, only sperm from cauda epididymis are susceptible to *in vitro* sperm capacitation. The apical acrosome is lost during acrosome reaction and this phenomenon could introduce modifications in the fluorescence signal.

In this study, prefixed sperm were incubated sequentially with lipid probes and FITC-PSA. Non-capacitated caput (data not shown) and non capacitated cauda sperm showed a predominantly *acrosomal* pattern by FIL and CTB probes (Figure 6, row A, picture b and c). Isothiocyano-fluoresceinated *Pisum sativum* (*Edible pea*) agglutinin shows an *acrosomal-cap* pattern indicating that the sperm does not undergo acrosome reaction (Fig. 6, row A, picture d). Interestingly, the confocal image from the same cell shows a good co-location (Figure 6, row A, picture e).

Capacitated cauda spermatozoa showed a decrease in the CHL fluorescent signal described here as the *diffuse* pattern (Compare Figure 6 row A picture b with row B picture g) and there is a redistribution of the GM1 fluorescence signal to the apical acrosome (Figure 6, row

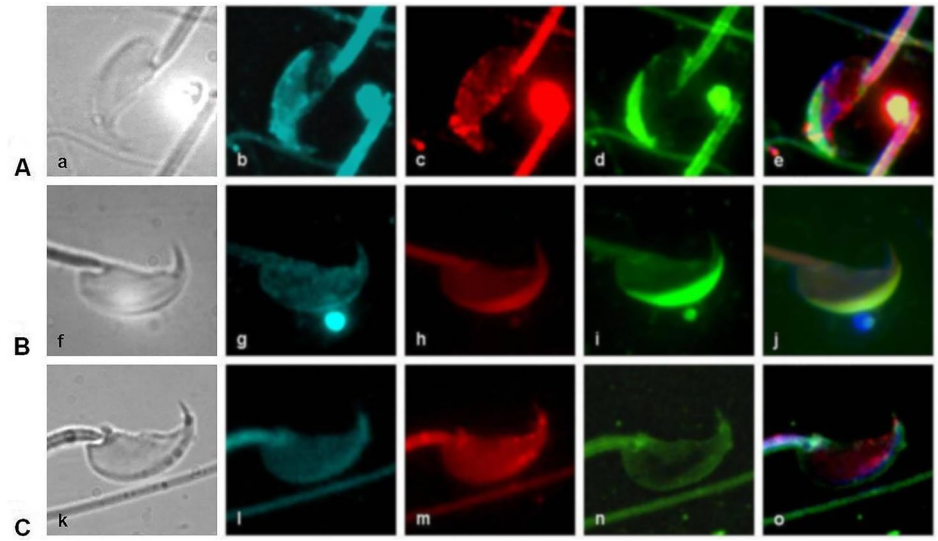

Figure 6: Lipids and acrosome reaction. Non-capacitated cauda sperm (A) show acrosomal patterns by FIL (b) and CTB (c) fluorescence probes, while acrosome apical is non-reacted. Capacitated cauda sperm (B) shows FIL diffuse pattern (g) and CTB acrosomal-cap pattern (h). Intact acrosome can be observed by FITC-PSA labelling under both incubation conditions (d-i). Acrosome reacted cauda sperm (C) maintains an FIL diffuse pattern (l). The CTB acrosomal pattern changes to diffuse pattern (m), coincident with the loss of the acrosome apical observed by FITC-PSA (n). The corresponding phase contrast (a, f and k) and merge (e, j and o) images are shown in each row.

B picture h). As it was stated previously, CHL was loss and GM1 redistributed to apical acrosomal region (*acrosomal-cap* pattern). Both fluorescence signals did not co-located in capacitated cauda sperm. In this case, the FITC-PSA signal has *acrosomal-cap* pattern (Figure 6, row B, picture i) indicating acrosomal integrity (unreacted), which co-localized with the GM1 (Figure 6, row B, picture j).

After PG or A23187 treatment, *diffuse* pattern observed by FIL probe did not change (Figure 6, row C, picture l), while *acrosomal-cap* pattern of GM1 observed in the capacitated cauda spermatozoa changed to *diffuse* pattern in the whole head (Figure 6, row C, picture m). This *diffuse* pattern of GM1 was only observed in capacitated sperm that underwent acrosome reaction confirmed by the loss of the FITC-PSA fluorescence signal (Figure 6, row C, picture n). During acrosome reaction the three signals did not co-localized on the head (Figure 6, row C, picture o). Table 2. Table 2 includes relative counts (percentage) of GM1 distribution described by CTB probe in *prefixed* cauda sperm under non capacitating condition, sperm capacitation and acrosome reaction.

These results indicate that lipid rafts in spermatozoa undergo changes across epididymal transit (maturation), sperm capacitation and acrosome reaction. Cholesterol maintains its acrosomal location (*acrosomal* pattern) in immature cells, whereas during sperm capacitation there was loss (*diffuse* pattern). Ganglioside GM1 during epididymal transit has *acrosomal* distribution as the CHL. After sperm capacitation, *acrosomal cap* pattern predominates for GM1. During acrosome reaction GM1 *acrosomal cap* pattern disappears as well as FITC-PSA signal, indicating acrosome exocytosis.

Discussion

A comparative study of CHL and GM1 distribution was performed to reflect their arrangement in the sperm plasma membrane. The simultaneous study of two components of the lipid domains (CHL and GM1) by specific probes (FIL and CTB) during maturation, sperm capacitation and acrosome reaction was analyzed here. Thus, the co-location of lipids permits us to introduce the idea of the disruption of rafts during sperm capacitation and acrosome reaction, in contrast with previous reports, in which the location of lipids was studied independently and this behaviour was not detected.

Furthermore, important assays were employed to establish the sperm capacitation status; the detection of p-Y and the detection of acrosomal reaction by Coomassie blue staining. Complementary to these methods, FITC-PSA labeling was used to study behavior both lipids during acrosome reaction in capacitated spermatozoa. The combination of these methods in the same population of cells allows us to detect whether changes are due to physiological conditions, or dead sperm and/or methodological artifacts.

In this paper mainly observed a strong fluorescence signal in the head acrosome domain (*acrosomal* pattern) by FIL (CHL) and CTB (GM1) in non capacitated sperm from caput and cauda epididymis under both fixing conditions. Thus, through standard fixation methods, CHL and GM1 do not show a visual redistribution during the epididymal transit. However, after *in vitro* sperm capacitation or, more dramatically, the induced acrosome reaction, both lipids showed intense changes in their specific locations.

In capacitated cauda spermatozoa, CHL showed weak fluorescence in the whole head with FIL probes (*diffuse* pattern), indicating its loss from the plasma membrane. Interestingly, CHL did not show significant differences of fluorescence pattern with FIL between *postfixed* and *prefixed* sperm from caput and cauda epididymis under incubation conditions.

On the other hand, GM1 could be more sensitive to fixation methods, due to the different results observed in this paper and by other authors. In *prefixed* spermatozoa, GM1 showed changes in fluorescence pattern, from *acrosomal* to *acrosomal-cap* pattern between non capacitated and capacitated cauda cells; while the equatorial segment remained devoid of signal fluorescence for this glycosphyngolipid with CTB probes. However, *postfixed* cauda sperm labeled by CTB probe presented an *acrosomal-cap/postacrosomal* pattern and did not show

significant differences between non capacitated and capacitated sperm.

In *prefixative* and *postfixative* conditions, sperm cells described as *other* were not a frequent pattern observed and they could be transitional states that have not completed the maturation/capacitation process. Besides, flagella midpiece showed an important fluorescence signal with both lipid probes, and these were maintained in all experimental conditions.

Based on these observations, CHL and GM1 co-localized in epididymal sperm indicated a significant amount of both components in the acrosome domain, which were maintained during maturation. These results indicate that lipid rafts are defined from the spermatogenesis and they experiment important physiological changes during sperm capacitation and the acrosome reaction.

In the sperm, these high levels of CHL could be important to maintain a non capacitating condition in the epididymis through the balance between activation and the suppression of membrane signalling processes [27,50]. Sperm capacitation can be induced *in vitro* in sperm from cauda epididymis. However, sperm capacitation cannot be induced in caput cells, which may be caused by an inhibition of protein kinases and/or by the predominant CHL acrosomal in immature sperm [42,50].

Cholesterol plays a major role in the assembly of signaling protein complexes, allowing the activation of signal transduction. During sperm capacitation, CHL efflux triggers p-Y of capacitation-specific proteins [14]. In the present work, the decrease of CHL during sperm capacitation can be observed as a *diffuse* pattern detected by FIL probe. This evidence of CHL efflux is also reported by other authors using cryofracture and fluorescence methods [25,51,52].

However, GM1 behavior has been largely discussed because of the different results reported in the literature. For example, in non capacitated sperm from boar and mouse, GM1 was observed principally over the tail, and following the CHL efflux, it diffused progressively toward the sperm head with the exception of the equatorial segment [27]. In contrast, Kawano [21] reported a postacrosomal pattern in non capacitated mouse sperm. In the uterine cavity, GM1 shifted from postacrosomal region to the equatorial segment, and this location disappeared in the oviduct, site where the acrosome reaction occurs. The reason for these results could be because the sperm were incubated with CTB before treatment with PF.

Also in mouse was suggested that GM1 localizes to the postacrosome domain and this localization does not change during sperm capacitation [26]. Some of these differences observed may be due to that these studies were performed at 16°C, which is lower than the physiological temperature.

Jones et al.[13] observed that GM1 was first accumulated on apical acrosome region and then diffused to the equatorial segment in live boar sperm. The meaning of this movement should be elucidated further; because studies in live cells are those that present the largest number of differences in localization and behavior about lipid rafts.

Consequently, these different findings reported about GM1 depend on the experimental conditions: live sperm or under fixative methods.

In the present investigation, experimental assays were performed *in vitro* under conditions equivalents to physiologic environment; in order to reduce the presence of technical artifacts.

For sperm capacitation, several molecules have been used because of their ability to extract CHL from the plasma membrane. For example, methyl-β-cyclodextrin (MBCD) enhances capacitation and induces phosphorylation. However, lipid diffusion rates and sperm capacitation are affected when MBCD-mediated CHL efflux is excessive [27].

Bovine serum albumin is other molecule used in *in vitro* sperm capacitation. Albumin is present in the female tract and is responsible for the removal of CHL from the sperm plasma membrane during sperm capacitation [53-57]. Furthermore, calcium and $NaHCO_3$ are also important female tract components. Visconti et al. [10] reported that BSA, Ca^{2+}, and $NaHCO_3$ in the medium are promoters of p-Y of multiple sperm proteins. For this reason, in the present study, cells were incubated in albumin (*in vitro* sperm capacitation by BSA), due to its physiological role as an essential molecule in sperm capacitation.

Also the fixative methods are critical for the analysis of lipid rafts. Selvaraj et al. [18] reported that live murine sperm incubated under non-capacitated condition, GM1 was found exclusively in the acrosome. Moreover, it was demonstrated that upon the cessation of motility or cell death in unfixed or lightly fixed sperm, GM1 moved from the acrosomal to the postacrosomal domain. This result suggests that a weak fixation is sufficient to immobilize sperm, but it is not adequate to immobilize GM1. The use of 4% PF plus 0.1% glutaraldehyde is adequate to immobilize lipids in the membrane sperm regardless of the incubation conditions [52-57]. In the present paper, similar results were obtained with 4% PF without the addition of glutaraldehyde.

A *postfixative* condition was employed as an alternative to study living sperm, allowing using specific fluorescence probes in unfixed cells. In this way the artifacts produced by the fixation technique could be avoided. However, this alternative *postfixative* condition may not be completely appropriate to study lipid changes in live sperm, possibly due to an alteration in the membrane composition.

In this investigation, successive centrifugation treatments did not produce a significant difference in the vitality in prefixed spermatozoa. However cells inevitably suffered some degree of stress when cells were previously labeled with specific probes and then fixed by PF. The degree of stress can be easily observed as *postacrosoma*l and *acrosomal-cap/ postacrosomal* patterns, predominant for GM1under *postfixatived* condition. These patterns were described above as dead cells.

As previously mentioned, lipids of membrane do not undergo changes through epididymal transit. One likely reason for the lipid behavior could be their interaction with other molecules present in the plasma membrane. The molecular barriers formed by transmembrane proteins between the equatorial segment with apical acrosomal region and postacrosomal domain have an important role in the lipid balance [58]. Single molecules are free to exchange across this barrier, but larger complexes are unable to do so [59]. The signalling complex might show polarized migration under physiological conditions from regions where they are inactive to areas where they become fully functional. This barrier is stabilized by the cytoskeleton, which is sensitive to intracellular changes that could affect the migration of polarized molecular complexes [59].

On the other hand, many studies have documented an interaction between a lipid raft-specific protein such as caveolin 1 (Cav1) and various signaling molecules present in membrane microdomains [60]. During sperm capacitation, Cav1 changes its membrane distribution from the acrosome domain to the apical acrosome region [61]. A similar GM1 description by CTB probe was observed in *prefixed* capacitated sperm in the present investigation.

GM1 ganglioside and Cav1, two components of the membrane microdomains, might be associated with the actin cytoskeleton during sperm capacitation and participate in acrosome reaction [62]. In the present work, the relationship between GM1 and acrosome reaction was studied by FITC-PSA labelling in *prefixed* capacitated sperm. *In vivo*, the zona pellucida stimulates the spermatozoa to undergo acrosome reaction. Calcium ionophore A23187 and PG are used to induct an *in vitro* acrosome reaction. Non-capacitated cauda sperm showed *acrosomal-cap* pattern with FITC-PSA, while capacitated cells incubated with several acrosome reaction inducers showed a characteristic *diffuse* pattern.

Reacted sperm showed a *diffuse* pattern with the three specific probes, indicating CHL efflux by FIL, early redistribution to acrosomal-cap domain and subsequent loss of GM1 signal by CTB, and acrosome reaction by FITC-PSA. These findings might indicate that there is a dynamic behavior in lipid rafts, which could be employed to the correlation between morphology and function. Moreover, in this investigation, it is observed that the method applied is critical when interpreting the results of studies about lipid rafts and their changes during the epididymal transit (sperm maturation), sperm capacitation and acrosome reaction. Spermatozoa under *postfixative* conditions presented different results. These differences were most noticeable for GM1.

Results exposed in this investigation showed a redistribution that could be correlated with the physiological changes of other raft components like Cav1, as well as an association with actin cytoskeleton.

Conclusion

This paper is a clear demonstration that sperm capacitation and acrosome reaction produce a redistribution of the lipids. However, there were no changes in lipid rafts during sperm maturation, possibly to avoid early sperm capacitation. Cholesterol efflux, a characteristic event of sperm capacitation, could be analyzed through the *diffuse* pattern described by FIL probes; and GM1 fluorescence patterns observed by the CTB probe could be interesting when it is needed to evaluate sperm capacitation and the acrosome reaction under *prefixed* conditions.

Acknowledgement

The authors are grateful to Prof. Amanda Vincenti, Mr. Alejandro Sabes, Prof. Gladys Costanzo and Rolando Damico for their technical support and English grammar assistant.

References

1. Alonso M, Millán J (2001) The role of lipid rafts in signaling and membrane trafficking in T lynphocytes. J Cell Sci 114: 3957-3965.
2. Lingwood D,Simons K(2010) Lipid rafts as a membrane-organizing principle. Science 327: 46-50.
3. Boerke A, Tsai P, Garcia-Gil N, Brewis I, Gadella B (2008) Capacitationdependent reorganization of microdomains in the apical sperm head plasma membrane: functional relationship with zona binding and the zona-induced acrosome reaction. Theriogenology 70: 1188–96.
4. Yanagimachi R (1994) Mammalian fertilization. In Knobil E, Neill JD (eds.). The physiology of reproduction. New York. Raven Press, pp: 189-317.
5. Chang M (1951) Fertilizing capacity of spermatozoa deposited into the fallopian tubes. Nature 168: 697-698.
6. Austin C (1952) The capacitation of the mammalian sperm. Nature 170: 326.
7. Seshagiri P, Mariappa D, Aladatti R (2007) Tyrosine phosphorylated proteins in mammalian spermatozoa: molecular and functional aspects. Soc Reprod Fertil Suppl 63: 313-25.
8. Gadella B, Evans JP (2011) Membrane fusions during mammalian fertilization. Adv Exp Med Biol 713: 65-80.
9. Gadella B, Luna C (2014) Cell biology and functional dynamics of the mammalian sperm surface. Theriogenology 8: 74-84.
10. Visconti P, Krapf D, de la Vega-Beltrán J, Acevedo J, Darszon A (2011) Ion channels, phosphorylation and mammalian sperm capacitation. Asian Journal of Andrology 13: 395-405.
11. Cooper T (1998) Interactions between epididymal secretions spermatozoa. J Reprod Fert Suppl 53: 119-136.
12. Dacheux J, Druart X, Fouchecourt S, Syntin P, Gatti J, et al. (1998) Role of epididymal secretory proteins in sperm maturation with particular reference to the boar. J Reprod Fert Suppl 53: 99-107.
13. Jones R (1998) Plasma membrane structure and remodelling during sperm maturation. J Reprod Fert Suppl 53: 73-84.
14. Visconti P, Bailey J, Moore G, Pan D, Olds-Clarke P, et al. (1995a) Capacitation of mouse spermatozoa. I. Correlation between the capacitation state and protein tyrosine phosphorylation. Development 121: 1129-1137.
15. Visconti P, Moore G, Bailey J, Leclerc P, Connors S, et al. (1995b) Capacitation of mouse spermatozoa. II. Protein tyrosine phosphorylation and capacitation are regulated by a cAMP-dependent pathway. Development 121: 1139-1150.
16. Salicioni A, Platt M, Wertheimer E, Arcelay E, Allaire A, et al. (2007) Signalling pathways involved in sperm capacitation. Soc Reprod Fertil Suppl 65: 245-259.
17. Munro S (2003) Lipid rafts: elusive or illusive? Cell 115: 377-388.
18. Selvaraj V, Buttke D, Asano A, Mcelwee J, Wolff C, et al. (2007) GM1 dynamics as a marker for membrane changes associated with the process of capacitation in murine and bovine spermatozoa. J Androl 28: 588-599.
19. Selvaraj V, Asano A, Buttke D, Sengupta P, Weiss R, et al. (2009) Mechanisms underlying the micrón-scale segregation of cholesterol and GM1 in live mammalian sperm. J Cell Physiol 218: 522-536.
20. Selvaraj V, Asano A, Buttke D, McElwee J, Nelson J, Wolff C, et al. (2006) Segregation of micronscale membrane sub-domains in live murine sperm. J Cell Physiol 206: 636-646.
21. Kawano N, Yoshida K, Iwamoto T, Yashida M (2008) Ganglioside GM1 mediates decapacitacion effects of SVS2 on murine spermatozoa. Biol Reprod 79: 1153-1159.
22. Friend D (1982) Plasma-membrane diversity in a highly polarized cell. J Cell Biol 93: 243-249.
23. Pelletier R, Friend D (1983) Development of membrane differentiations in the guinea pig spermatid during spermiogenesis. Am J Anat 167: 119-141.
24. Suzuki F (1988) Changes in the distribution of intramembranous particles and filipin-cholesterol complexes during epididymal maturation of golden hamster spermatozoa. J Ultrastruct Mol Struct Res 100: 39-54.
25. Lin Y, Kan F (1996) Regionalization and redistribution of membrane phospholipids and cholesterol in mouse spermatozoa during in vitro capacitation. Biol Reprod 55: 1133-1146.
26. Treviño C, Serrano C, Beltrán C, Felix R, Darszon A (2001) Identification of mouse trp homologs and lipid rafts from spermatogenic cells and sperm. FEBS Lett 509: 119-125.
27. Shadan S, James P, Howes E, Jones R (2004) Cholesterol efflux alters lipid raft stability and distribution capacitation of boar spermatozoa. Biol Reprod 71: 253-265.
28. Roberts K, Wamstad J, Ensrud K, Hamilton D (2003) Inhibition of capacitation-associated tyrosine phosphorylation signaling in rat sperm by epididymal protein Crisp-1. Biol Reprod 69: 572–581.
29. Cross N (2004) Reorganization of lipid rafts during capacitation of human sperm. Biol Reprod 71: 1367-1373.
30. Lee M, Storey B (1986) Bicarbonate is essential for fertilization of mouse eggs: Mouse require it to undergo the acrosomal reaction. Biol Reprod 34: 349-356.
31. Cohen D, Ellerman D, Cuasnicú P (2000) Mammalian sperm-egg fusion: evidence that epididymal protein de plays a role in mouse gamete fusion. Biol Reprod 63: 462-468.
32. World Health Organization (WHO) Laboratory Manual for the Examination and

Processing of Human semen (2010) Cambridge. Cambridge University Press, pp. 52.

33. Laemmli U (1970) Cleavage of structural proteins during the assembly of the head of bacteriophage T4. Nature 227: 680-685.

34. Towbin H, Staehelin T, Gordon J (1979) Electrophoretic transfer of proteins from polyacrylamide gels to nitrocellulose sheets: procedure and some applications. Proc Natl Acad Sci USA 76: 4358-4364.

35. Tabas I, Zha X, Beatini N, Myers J, Maxfield F (1994) The actin cytoskeleton is important for the stimulation of cholesterol esterification by atherogenic lipoproteins in macrophages. J Biol Chem 269: 22547-22556.

36. Boarelli P, Cattaneo C, Monclus M, Fornés M (2007) Detección de la capacitación espermática basada en la visualización de los componentes lipídicos de microdominios de membrana. Rev Med Univ 3: 1-11.

37. Asano A, Selvaraj V, Buttke D, Nelson J, Green K, et al. (2009) Biochemical characterization of membrane fractions in murine sperm: identification of three distinct sub-types of membrane rafts. J Cell Physiol 218: 537–548.

38. Saez Lancellotti T, Boarelli P, Monclus M, Cabrillana M, Clementi M, et al. (2010) Hypercholesterolemia impaired sperm functionality in rabbits. PLoS One: e13457.

39. Jones R, Howes E, Dunne P, James P, Bruckbauer A, et al. (2010) Tracking diffusion of GM1 gangliosides and zona pellucida binding molecules in sperm plasma membranes following cholesterol efflux. Develop Biol 339: 398–406.

40. Wolf D, Voglmayr K (1984) Diffusion and regionalization in membranes of maturing ram spermatozoa. J Cell Biol 98: 1678-1684.

41. Wolf D, Maynard V, McKinnon C, Melchior D (1990) Lipid domains in the ram sperm plasma membrane demonstrated by differential scanning calorimetry. Proc Natl Acad Sci U S A 17: 6893-6896.

42. Christova Y, James P, Mackie A, Cooper T, Jones R (2004) Molecular diffusion in sperm plasma membranes during epididymal maturation. Mol Cell Endocrinol 216: 41-46.

43. Roldan E, Tetsuma M, Qi-Xian S (1994) Exocytosis in spermatozoa in response to progesterona and zona pellucida. Science 266: 1578-1581.

44. Murase T, Roldan E (1996) Progesterona and the zona pellucida activate different transducing pathways in the sequence of events leading to diacylglycerol generation during mouse sperm acrosomal exocytosis. Biochem J 320: 1017-1023.

45. Pietrobon E, Domínguez L, Vincenti A, Burgos M, Fornés M (2001) Detection of the mouse sperm acrosome reaction by acid phosphatase. Comparison with chlortetracycline and electron microscopy. J Androl 22: 96-103.

46. Muñoz-Garay C, De la Vega-Beltrán J, Delgado R, Labarca P, Félix R, et al. (2001) Inwardly rectifying K1 channels in spermatogenic cells: functional expresion and implication in sperm capacitation. Dev Biol 234: 261-274.

47. Ozaki T, Takahashi K, Kawasaki H, Miyazaki K (2002) Evaluation of acrosome reaction and viability of human sperm with two fluorescent dyes. Arch Gynecol Obstet 166: 114-117.

48. Lybaert P, Danguy A, Leleux F, Meuris S, Lebrun P (2009) Improved methodology for the detection and quantification of the acrosome reaction in mouse spermatozoa. Histol Histopathol 24: 999-1007.

49. Yamashita M, Yamagata K, Tsumura K, Nakanishi T, Baba T (2007) Acrosome reaction of mouse epididymal sperm on oocute zona pellucida. J Reprod Develop 53: 255-262.

50. Harayama H (2013) Role of intracellular cyclic AMP signal transduction in the capacitation and subsequent hyperactivation of mouse and boar spermatozoa. J Reprod and Develop 9: 421-430.

51. James P, Wolfe C, Ladha S, Jones R (1999) Lipid diffusion in the plasma membrane of ram and boar spermatozoa during maturation in the epididymis measured by fluorescence recovery after photobleaching. Mol Reprod Dev 52: 207-215.

52. Takeo T, Hoshii T, Kondo Y, Toyodome H, Arima H, et al. (2008) Methyl-beta-cyclodextrin improves fertilizing ability of C57BL/6 mouse sperm after freezing and thawing by facilitating cholesterol efflux from the cells. Biol Reprod 78: 546-551.

53. Davis B, Byrne R, Hungund B (1979) Studies on the mechanism of capacitation. II. Evidence for lipid transfer between plasma membrane of rat sperm and serum albumin during capacitation in vitro. Biochim Biophys Acta 558: 257-266.

54. Davis B (1981) Timing of fertilization in mammals: sperm cholesterol/phospholipid ratio as a determinant of the capacitation interval. Proc Natl Acad Sci USA 78: 7560-7564.

55. Go K, Wolf D (1985) Albumin-mediated changes in sperm sterol content during capacitation. Biol Reprod 32: 145-153.

56. Langlais J, Zollinger M, Plante L, Chapdelaine A, Bleau G, et al. (1981) Localization of cholesteryl sulfate in human spermatozoa in support of a hypothesis for the mechanism of capacitation. Proc Natl Acad Sci USA 78: 7266-7270.

57. Suzuki F, Yanagimachi R (1989) Changes in the distribution of intramembranous particles and filipin-reactive membrane sterols during in vitro capacitation of golden hamster spermatozoa. Gamete Res 23: 335-347.

58. Bruckbauer A, Dunne P, James P, Howes E, Zhou D, et al. (2010) Selective diffusion barriers separate membrane compartments. Biophys J 99 : L1-3

59. Jones R, James P, Howes L, Bruckbauer A, Klenerman A (2007) Supramolecular organization of the sperm plasma membrane during maturation and capacitation. Asian J Androl 9: 438–444.

60. Fielding C, Fielding P (2004) Membrane cholesterol and the regulation of signal transduction. Biochem Soc Trans 32: 65-69.

61. van Gestel R, Brewis I, Ashton P, Helms J, Brouwers J, et al. (2005) Capacitation-dependent concentration of lipid rafts in the apical ridge head area of porcine sperm cells. Mol Hum Reprod 11: 583–590.

62. Liu P, Rudick M, Anderson R (2002) Multiple functions of caveolin-1. J Biol Chem 277: 41295-41298.